A System to Characterize Battery Behavior in Miniature Wildlife Tags Reveals Correctable Reliability Weaknesses

December 19, 2018

Abstract

We describe a system that we have designed, built, and used to investigate the behavior of small batteries that power miniature wildlife tracking tags. The system enables simple and low-cost long-term (days to weeks) monitoring of tags powered by such batteries, as well as testing batteries under a simulated tag load. Using this system, we have found a major cause of failures in tags, an effect called *concentration polarization*, which causes a transient increase in the internal resistance of the battery. The paper describes the rationale and design of the system, the failures that we have discovered using it, and several mechanisms that we have assessed to mitigate this effect as well as the naturally-high internal resistance of miniature batteries.

1 Introduction

Powering miniature wildlife tags remains a significant challenge, even after more than a half-century of experience with such tags. There are several reasons that this problem has not been resolved. First, modern wildlife tags are based on CMOS digital electronic that require at least 1.8V, whereas some cell chemistries only deliver around 1.5V, requiring a pair of batteries (silver oxide and zinc air) or a DC-DC boost converter. Second, many miniature batteries cannot deliver the peak current that transmitting tags require, often around 20mA; this is true both for radio transmitters and for ultrasonic transmitters, which are used to track fish. Third, the market for suitable batteries is small and fragmented, limiting commercial interest in the development of batteries that better match the requirements. Fourth, the processes inside batteries are complex and can lead to tag failure even when if the voltage and peak current requirements are met.

In particular, users of tags designed by one of the authors complained that a non-trivial number of tags have failed, with a variety of batteries, including both miniature batteries and larger ones (e.g., AA size lithium cells), in spite of a careful study to characterize batteries that should work well with the tags [10], and in spite of an on-tag mechanism designed to mitigate such problems (a reservoir or bulk capacitor [11, 10]).

Trying to replicate and study these failures in the lab proved difficult. In some cases, tag failure quickly depleted one battery but when we attached the tag to another battery of the same type, it performed flawlessly. In other cases, we were able to replicate failures, but capturing all the relevant voltages and currents at the time of failure on an oscilloscope proved difficult.

These user-reported failures and the difficulty of diagnosing them motivated the research reported here. We decided to build a specialized but easy-to-replicate test instrument that would allow us to address the following problems

- The instrument should allow us to capture all the relevant current and voltage measurements around to the time of failure, both before and after the failure.
- The instrument should allow us to perform large-scale testing of batteries, both when they power actual tags and when supplying simulated loads.

We also felt that an easy-to-replicate test instrument could also achieve additional goals, which are less critical but still useful:

- Users (biologists and their technicians) should be able to use it to perform the same types of analyses.
- Users should be able to use the instrument to measure the life spans of tags with different configurations (transmission rates and power, etc) and different batteries.
- Users should be able to monitor the current consumption of tags using the instrument. This monitoring can be done using an oscilloscope and a current-sensing resistor, but not all tag users have an oscilloscope, setting up the scope to monitor current consumption is non-trivial (not difficult to frequent users of oscilloscopes, but non trivial for casual users). The instrument is also considerably less expensive than an oscilloscope.

The instrument and the software system that drives it have indeed enabled us to discover an important cause of failures that we were not aware of. To the best of our knowledge, has not been described in the literature on the design of wildlife tracking and sensing tags. The system also allowed us to assess mitigation mechanisms intended to eliminate this cause of failure. We found that one mechanism mitigates but does not completely eliminate the problem; another appears to address it fully. Briefly, we discovered that miniature lithium coin cells sometimes suffer from *concentration polarization*, an effect that raises the internal resistance sigificantly but temporarily. We also discovered that limiting from below the impedance that the battery sees (to a value in the single kilo-Ohms range) reduces the frequency of this effect but does not eliminate it completely; by skipping activity period while the internal resistance is high, tags should be able to survive these transients, allowing the battery to recover (through diffusion of the reactants).

Two other contribution of the paper are an analytic technique to size both the reservoir capacitor and the current-limiting resistor, and a circuit to disconnect the reservoir capacitor when the tag is in so-called *ship mode* (as inactive as possible, to extend shelf life) and to reconnect it safely when the tag is pressed into service.

The rest of this paper is organized as follows. Section 2 provides background on this problem. Section 3 describes the characterization system that we designed. Section 5 shows how to limit the impedance that the battery sees and how to size the reservoir capacitor and the current-limiting resistor. Section 6 describes a technique to safely connect and disconnect the reservoir capacitor. Section 7 describes the results of experiments in which the tag skips activity pulses when the battery's impedance might be too low, risking a reset or failure. We present our conclusions from this research in Section 8.

2 Background

Almost all wildlife tags today use a microcontroller; many also contain a radio transmitter or transceiver or an ultrasonic transducer, sometimes sensors, and sometimes an additional memory chip. Early radio tag designs [3] were completely analog and are easier to power, but are outside the scope of this paper; similar designs are still used quite widely [8]. Integrated circuits that are appropriate for wildlife tags require at least 1.8V (often 1.8 to 3.6 or 3.8V). Transmitting a low-power radio signal from an integrated transceiver usually requires 10mA or more; powering a GPS receiver requires even more, often around 30mA. Relatively large Lithium primary batteries can provide the required voltage and current, but small Lithium coin cells and other miniature batteries (e.g., silver oxide) cannot provide enough current or they may struggle.

Toledo placed a range of miniature batteries under a load that simulates the behavior of a radio tag [10]. The simulator is programmed for a repetition rate, say 1Hz, pulse duration, say 8ms, and current, say 35mA. The load sources the prescribed current for the prescribed pulse duration repeatedly. The battery voltage is sampled both during pulses and between pulses. Testing continues until the battery voltage under load drops below a certain value, say 1V; this value is often lower than the 1.8V threshold of actual tags, to show what happens as the battery empties.

This testing has revealed that silver-oxide batteries, the smallest available for tags, cannot supply enough current. When the battery is connected to the tag in parallel with a large capacitor (the paper used 1000μF), the load was able to source the required current; the current during the pulse was provided by the capacitor, which was recharged by the batteries before the next pulse. Reservoir capacitors have been used in a number of recent tag designs. For example, Deng et al. used one in an acoustic ultrasound tag; they write "a bulk capacitor smooths the large current pulse that occurs during transmission to prevent damage to the battery" [4]. They do not explain what damage would occur without this capacitor. Dressler et al. describe a lightweight wildlife tag that uses a capacitor "to provide peak operating current for the system" because the primary Lithium coin cell can only deliver about 0.5 mA, not enough to power the tag when the radio is active [5].

This laboratory characterization of batteries by Toledo yielded a number of other conclusions [10], some that held up in the field and some that did not. The data showed that a pair of zinc air batteries could easily power tags, at least if the tag is not submerged in water; in the field, these batteries proved unreliable and users do not use them. The data also showed that

the reservoir capacitor can extend the operational life span of tags powered by batteries that do not absolutely need the capacitor, such as Lithium CR1632 cells. Finally, the data showed some voltage drops that were not explored fully [10, Figure 5]; these were not fully explored. Similar voltage drops in other experiments not presented in the paper were thought to be the result of defective batteries.

When a reservoir capacitor connected in parallel with battery, the voltage at the battery-capacitor node can drop during a pulse. The voltage drops if the internal resistance of the battery allows the capacitor to become partially discharged. When the voltage in that node is lower than the battery's voltage at rest, the battery sees a very low impedance load. Based on some unreported and incomplete testing, Toledo became concerned that this might cause damage to silver oxide batteries; to prevent that, he included a current-limiting capacitor between the silver-oxide cells and the reservoir capacitor in the tags he designed since 2015. He instructed users to connect silver-oxide batteries to the tag through that resistor, after the tag has been "jump started" by connecting a low-internal resistance power source directly to the capacitor (e.g., a pair of AA alkaline cells); he informed users that Lithium coin cells can be connected in parallel with the capacitor.

It appears that other researchers were also concerned about the effect of the low impedance of the capacitor. For example, Dressler et al. present a block diagram of their tag, showing that the battery is connected to the capacitor through a current-limiting resistor [5]. They do not discuss or explain the function of this resistor.

Obviously, the chemistry literature on the characteristics of batteries is vast, but is difficult in general for circuit and system designers to understand. Martin provides a good overview of battery characteristics for this audience [7, Appendix C].

The mismatch between available batteries and the requirements of wildlife tags can also be addressed by designing better-matched batteries. Chen et al. [2] describe such a project. The battery that they designed for ultrasonic fish tags can probably be successfully used on radio tags, but it is not available commercially, even though the design has been licensed to a company[1]; apparently, the company does not judge the market for the battery to be currently large enough.

3 Characterization System Design

To achieve our goals, we designed and built a system to characterize the behavior of miniature batteries under a real or simulated load that is typical for wildlife tracking tags. The system consists of hardware (an analog circuit interfaced to a microcontroller), firmware, and host software that drives the testing and collects the results. The system is an enhancement of a load simulation system built earlier by one of the authors to address some of our goals [10].

[1] Zhiqun (Daniel) Deng, personal communication.

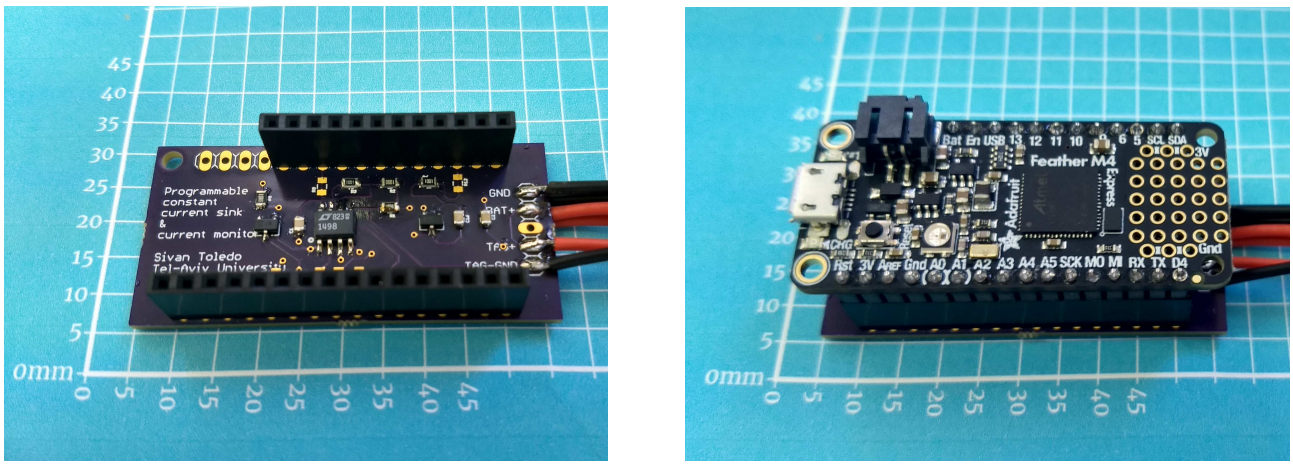

Figure 1: The battery characterization hardware. The image on the left shows the add-on circuit that we designed and built. The image on the right shows the same unit, but stacked below an Adafruit Feather M4 Express microcontroller board.

3.1 Platform

We chose to build the hardware around a microcontroller board with a fairly fast ARM processor and with a small form factor (24 by 51mm). The board is the *Adafruit Feather M4 Express* board, with an 120MHz Cortex M4 microcontroller (ATSAMD51J19) with and 512KB Flash and 192KB RAM. The feather series consists of boards with several different microcontrollers, some with WiFi or other radios and with extension connectors that have the same or almost the same layout in all the boards. Therefore, extension boards like the one that carries our analog circuit can be compatible with multiple feather boards. Ours is compatible at least with the Express M4 board and with the WICED WiFi board, costing $23 and $35, respectively.

These feather boards support the Arduino firmware environment, which is an easy-to-use C++ programming environment that supports numerous microcontroller boards. The Express M4 board also supports CircuitPython, a more high-level firmware environment. We used the Arduino environment. We selected it for performance (it produces native C/C++ binaries), because it allows our firmware to run on many other microcontroller boards, and because it allows others to earily modify and enhance our code (it is more highly standardized and widely used than any other firmware environment).

The small form factor of the feather boards makes the hardware unit compact and reduces the cost of the analog circuit board. The size still allows for easy manual assembly of the custom analog board (one of the authors manually soldered 11 of these boards in a few hours).

3.2 Hardware Design

The analog part of our load tester and battery simulator is shown in Figure 2. The middle part featuring opamp IC1A is a programmable current sink that is used as a load simulator. It is almost identical to the load simulator described in [10], with the exception of C16. In general, when Q2 is not conducting (pin 5 is low), the opamp and Q1 force current to flow through R5 such that the voltage drop on it is equal to the voltage in the inverting pin of opamp IC1A, which is driven

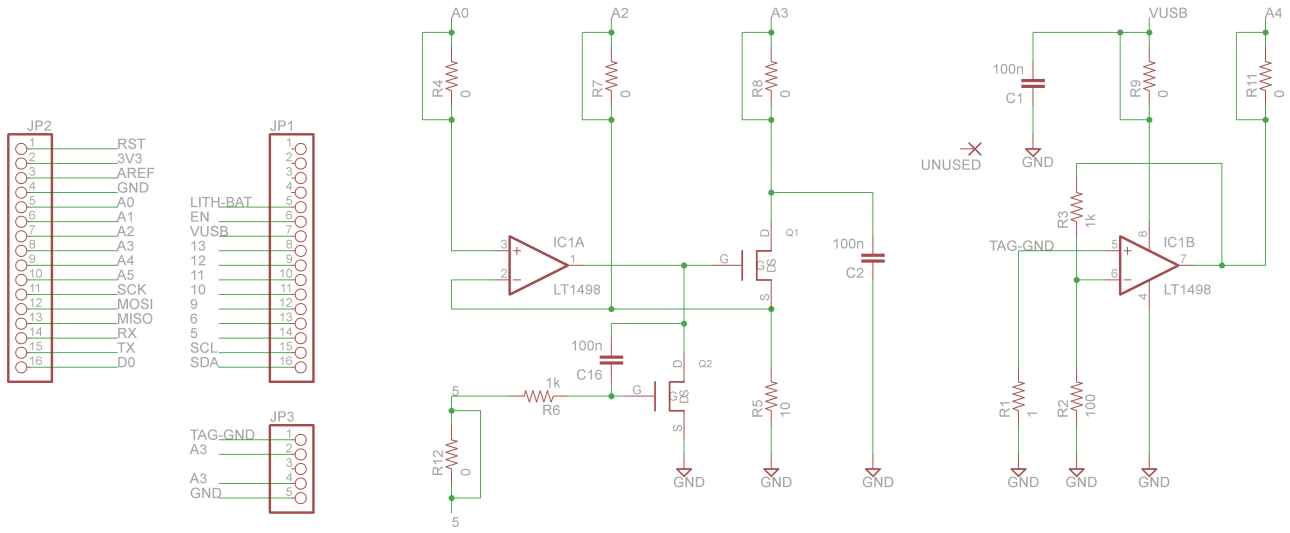

Figure 2: The circuit of the load simulator and battery tester. Connectors JP1 and JP2 connect the circuit to microcontroller board from the Adafruit feather series. Connector JP3 is used to connect the battery under test and possibly a tag. Pin A0 is used to set the current that the simulator draws from the battery in each pulse; it should be driven by a DAC. Digital pin 5 controls the current sink; when low, the simulator draws current from the battery, when it is high, the simulator draws no current (but the tag might, if one is connected). Pin A2 should be connected to an ADC; it monitors the current drawn by the simulator. Pin A3 monitors the battery voltage. Pin A4 monitors the current drawn by the tag.

by a digital-to-analog converter (DAC).

The role of capacitor C16, which was missing the original load simulator, is to enhance the Miller effect of MOSFET Q1, in order to slow down the turn-on of the current sink. Without it, the current drawn by the load starts with a high short (on the order of a microsecond) spike that settles to the programmable level. This spike, which does not occur under actual loads, can potentially stress the battery. The spike is part of the settling of the opamp circuit, in which the negative feedback loop is open before the pulse (the gate of Q1 is grounded).

Spice simulation indicates that without this Miller capacitor, a 35mA current-sinking pulse starts with a 270mA spike lasting 1.5μs. With the 0.1μF capacitor, the spike reduces to 40mA. Oscilloscope measurements verified these findings. The details of the spike depend on the parameters of both the MOSFET and the opamp; the simulation used the parts that we use in the actual circuit, DMN1019 and LT1498.

The circuit around IC1B is simply an 11× amplifier that amplifies the voltage developed across the current sensing resistor R1. The voltage drop across this resistor causes tags to fail while battery voltage is still above the tag's threshold (around 1.8V), but only slightly so, about 20mV above the threshold.

We also simulated another version of the circuit, in which both sections of the opamp formed a single feedback loop. In that variant, the tag is connected in parallel with Q2 (to its drain and source) and R1 is reduced to around 1 Ohm or lower. This required amplification of the voltage across R1. The potential advantage of this configuration is that it enables the use a single analog-to-digital (ADC) pin for both the load simulator and measurement of current drawn by actual tags.

However, this variant proved to be unstable in simulation mode. Since most microcontrollers have multiple ADC pins, the disadvantage of the two current-sensing outputs in the final design is negligible.

The function of the shorted zero-Ohm resistors that connect the circuit to the pins of the feather board was to allow patching the circuit, should modifications prove necessary (the shorting trace can be cut and the PCB pads for the SMD resistors can be used for patching wires). In other words, these are PCB features designed to make a prototype flexible. They have no function in the final design (and they proved unnecessary).

3.3 Firmware, Software and Protocol Design

The system can be used in one of two modes. In simulation mode, the experiment is driven by a host computer running C-sharp software that drives the experiment and collects measurement data. In observation mode, the system monitors the current consumption and battery voltage of an actual tag. In this mode, measurements are still transferred from the microcontroller to the host for storage, but the host has no control over the schedule of the experiment; the tag does.

In simulation mode, the user configures the pulse-repetition rate, the pulse duration, and the current to be drawn in each pulse. Each current-sinking pulse is initiated by the host. This ensures that if the host software stops or the host itself halts or reboots, the experiment is suspended and the battery is not drained further, until the experiment is restarted. This is important since some of these experiments, especially with large batteries, can last days or weeks. In this mode, the firmware waits for a command from the host to start a pulse. During this wait, it monitors battery voltage and records the highest voltage it has seen. When a command arrives, the firmware sets the DAC output to the correct level, starts the pulse by clearing pin 5, and samples the battery voltage and the current drawn at a high rate. The samples are time stamped. At the end of the pulse, the firmware sends to the host the highest voltage before the pulse (and resets this variable), the lowest voltage and highest current during the pulse, and all the samples of current and voltage during the pulse. The firmware samples the ADC at about 12.5kHz (this is a limitation of the Arduino library that drive the ADC; the microcontroller can sample at up to 1000ks/s), giving about 50 current samples and 50 voltage samples for an 8ms pulse.

In this mode, host software stores all the data in a file and can display both the overall graphs of extreme values in each pulse (highest voltage before the pulse, lowest voltage and highest current during the pulse), as well as the detailed measurements during a pulse that the user selects on the screen (this visualization software is written in Python).

In tag-testing mode, the firmware discovers the timing of current-drawing pulses automatically using a set of rules. The rule that indicates the beginning of a pulse requires 4 consecutive current samples to exceed a threshold of about 5.4mA; the rule for terminating a pulse is 4 samples below 4.5mA, to provide hysteresis. These thresholds are constrained by the opamp errors (mainly offset voltage), which are fairly high for the LT1498. A precision opamp should allow using much lower thresholds. At the end of each pulse, the firmware sends the same data as in simulation mode: extreme values before and during the pulse, high-resolution measurements during and just before

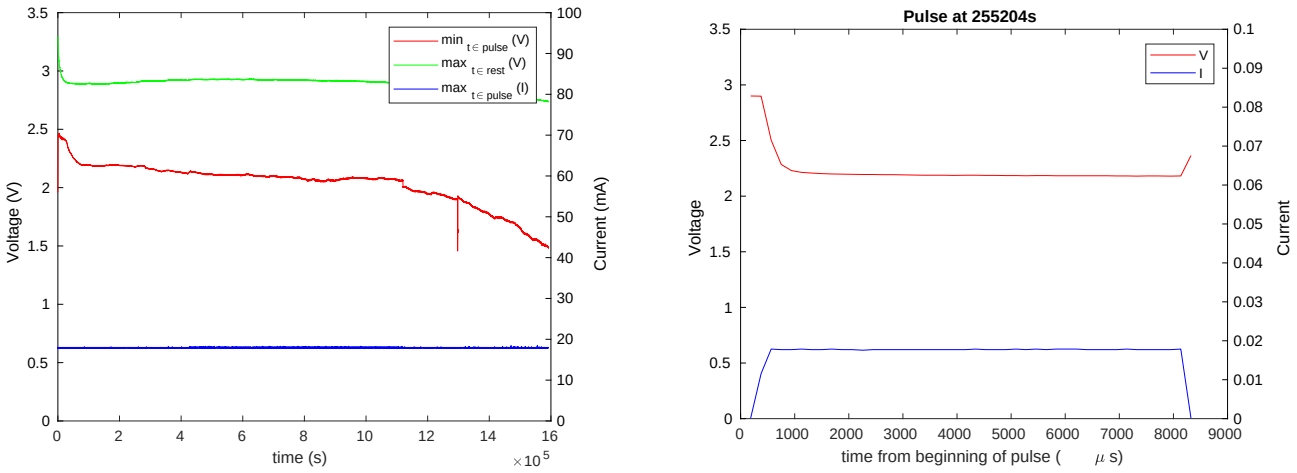

Figure 3: Behavior of Renata CR1625 battery. The apparent failure around second 1,250,000 was caused by a bad connection, not intrinsic battery behavior. The graph on the right shows the behavior during one pulse: while current is drawn, the battery's internal resistance causes voltage to drop, here by about 650mV, indicating an internal resistance of about 34 Ohms. We can clearly see the internal resistance rising as the battery drains.

the pulse. The firmware uses a 15-slots cyclic buffer to store pre-pulse measurements.

The tag-testing mode also implements facilities to record the current and voltage behaviors when a tag behaves abnormally, which is usually caused by some failure or fault. In normal behavior, tags consume current in short pulses that last up to 30ms or so (with a high consumption that is typically much shorter, around 8ms, sometimes followed by lower consumption for some additional time, to store sensor measurements or to perform other housekeeping activities). When a tag fail, it can consume current continuously, which can drain the battery. When a pulse lasts longer than a threshold (30ms), the firmware moves to slow-sampling mode, in which the tag reports every millisecond the maximal current and minimal battery voltage consumed in the previous millisecond. Host software records these values but can aggregate them if the failure lasts longer than a few seconds.

4 Initial Experimental Results: The Effect of Reservoir Capacitors

Our main finding is that small lithium coin batteries connected in parallel with reservoir capacitors sometimes fail catastrophically under tag-like loads. We tested a range of different Renata lithium coin batteries under a periodic constant current loads. The load drew about 19mA from the battery for 8ms every second.

Figure 3 shows the behavior of a CR1625 battery under this load. Due to its somewhat small size, the battery struggles to deliver 19mA; after a short while, voltage sags during the pulse by about 0.65, and the sagging gets worse and worse as the battery drains. Still, voltage stays above 1.8V for at least 1.2Ms. A tag with similar current consumption can be easily powered by this battery. However, the gradual increase in internal resistance will cause the voltage to sag below

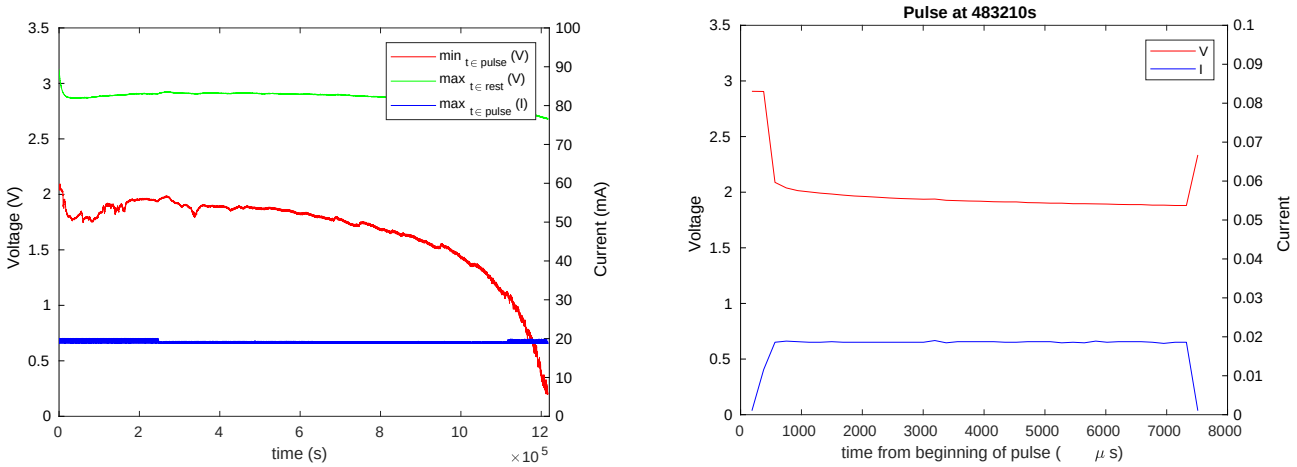

Figure 4: Behavior of Renata CR1225 battery under the same load. The internal resistance fluctuates; at best, the voltage under load is 2V (internal resistance of about 47 Ohms), but it is less even than in Figure 3 and dips close to or below 1.8V even when the battery is nearly full.

1.8V when there is still a significant amount of energy in the battery.

Figure 4 shows that a smaller battery, size CR1225, cannot power the tag reliably, at least not without a reservoir capacitor. The graphs show that the internal resistance (voltage sag) is higher, and that voltage sags near or below 1.8V even when the battery is still nearly full.

To overcome the high internal resistance of miniature batteries like CR1225 (and smaller ones, including lithium CR1025 and silver oxide cells), we and others have been using a reservoir capacitor large enough to supply enough current for one pulse on its own. To simulate this, we connected batteries in parallel with either a miniature 330μF tantalum capacitor, AVX F950J337KBAAQ2 [1] or a A miniature 330μF (nominal) ceramic capacitor, Taiyo Yuden JMK325ABJ337MM-P [9], both rated for 6.3V. The tantalum capacitor is 3.5 by 2.8 by 1.8mm and has maximum equivalent series resistance (ESR) of 0.6 Ohms (at 100kHz). The ceramic capacitor has effective capacitance of only 220μF from DC to about 100kHz, a strong reduction in capacitance at high DC bias (about 40% at 3V), and extremely low ESR, 1mOhm at 100kHz and about 10mOhm at 1kHz. The tantalum capacitor is used in most of the ATLAS and Vildehaye tags produced so far (see, e.g., [12]).

Figure 5 shown the normal behavior of CR1025 batteries connected in parallel with the two types of capacitors (one at a time) under this load. The ceramic capacitor causes the voltage to drop lower than the tantalum unit, even initially, because its effective capacitance is lower. The graphs also show two additional behaviors that we do not currently understand, but are not critical. The first is the gradual decrease in the capacitance of the ceramic capacitor, causing voltage under load to sag lower and lower. The other is variability in the lower voltage under load. Zooming in on the graphs reveals that this is a periodic phenomenon, in which the effective capacitance appears to vary cyclically. The voltage under load in these settings drops fairly linearly, as shown in Figure 6 (left), because the capacitor is discharged almost linearly (most of the charge is provided to the load from the capacitor, not from the battery that has a much higher resistance).

However, the capacitor can also stress the battery, causing a tag to fail. Figures 6 and 7 show such behaviors. In both cases, the battery experiences significant voltage drops, including in the

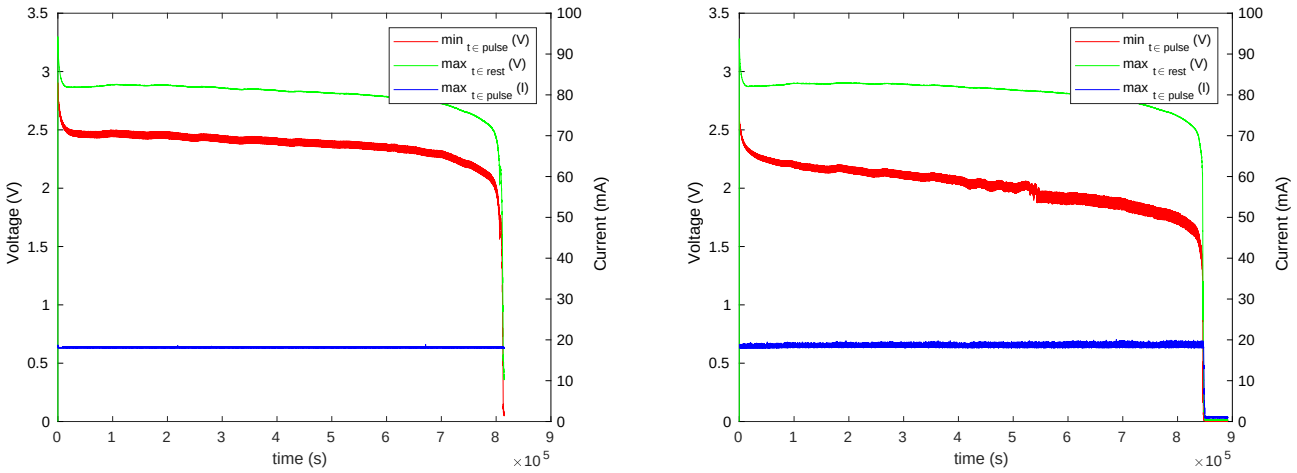

Figure 5: Behavior of Renata CR1025 batteries connected in parallel with a capacitor under pulsed load. The load simulator was programmed to draw about 20mA for 8ms every second. In the graph on the left, the capacitor was a 330μF tantalum capacitor; in the graph on the right, a 330μF (nominal) ceramic capacitor with effective capacitance around 220μF.

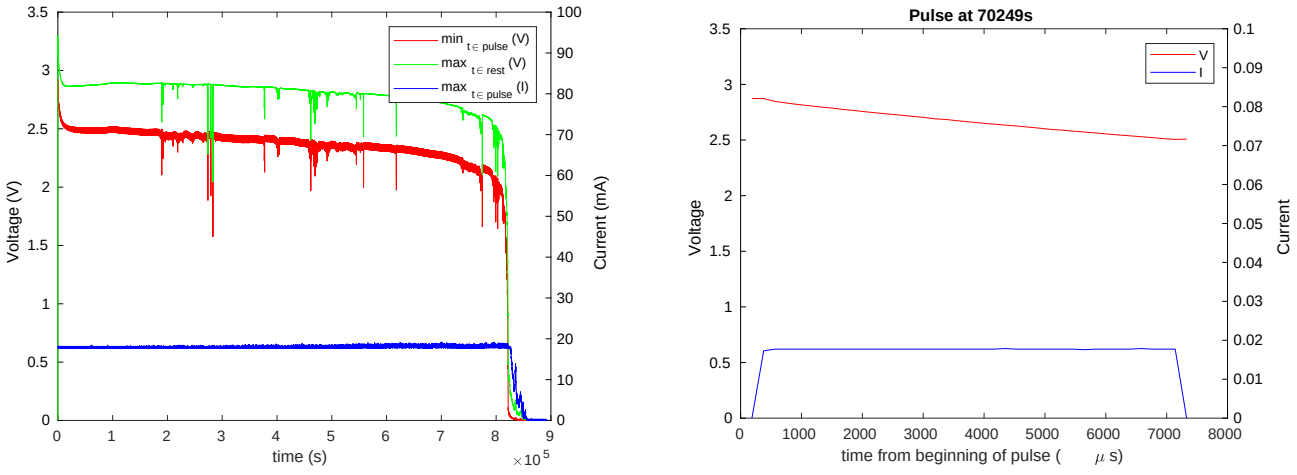

Figure 6: Behavior of Renata CR1025 battery in parallel with a tantalum capacitor, showing occasional voltage drops, at least one catastrophic (below 1.8V). The graph on the right shows the behavior within one pulse, at a time in which the battery behaved normally. The capacitor and the load were the same as in Figure 5.

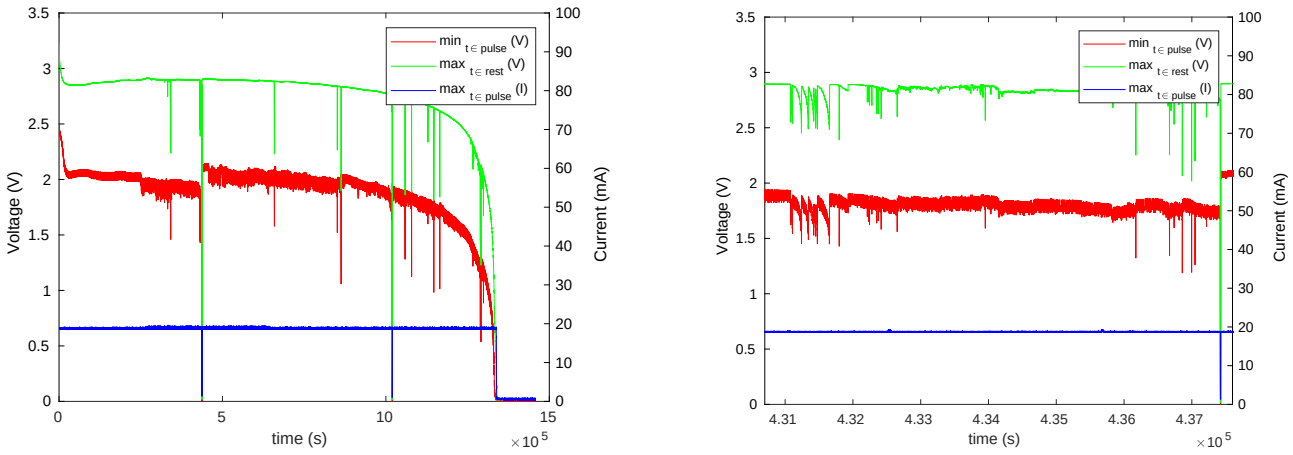

Figure 7: Behavior of Renata CR1225 battery in parallel with a ceramic capacitor, showing occasional voltage drops, many catastrophic (below 1.8V). The graph on the right zooms in, showing interesting patterns of failure after which the battery recovers. The capacitor and the load were the same as in Figure 5.

inter-pulse periods (that is, these failures last more than a second), and sometimes dropping well below 1.8V. The tantalum capacitor induced mostly single-pulse failures. The ceramic capacitor sometimes induces repeated prolonged periods in which the battery experienced difficulties, perhaps due to its much lower ESR.

These failures appear to be caused by a phenomenon called *concentration polarization*, in which internal resistance increases temporarily because reactants become depleted near the battery's electrodes (see, e.g., [7, 6]). This is resolved through diffusion of the reactants, hence resolution can be slow. This phenomenon can be caused by exposing the battery to a load impedance load, even for short periods[2]. These low-ESR capacitors indeed present a very low-impedance load to the batteries. As the pulse progresses, the capacitor is discharged because the tag or the simulator sinks more current than the battery can provide, so the voltage across the capacitor drops. This presents a very low impedance load to the battery.

These failures do not always occur. We repeated the tests with two identical fresh CR1225s, one with each capacitor type; failures were observed only in the battery connected to the ceramic capacitor. We then ran the experiment with two CR1025s connected to two identical tantalum capacitors and two CR1025s connected to two ceramic capacitors; the capacitors from the CR1225 experiments were reused. In the second experiment, only one battery failed, one connected to a tantalum capacitor. We conclude that the propensity for these failures depends on the individual battery; it is not uniform even for batteries from the same batch.

Figure 8 shows the behavior of a tag connected to a CR1225 battery in parallel with a tantalum capacitor. In general, the behavior is similar to that of the simulated load, except that the current consumption is smaller and varies more.

[2]Personal communication with Prof. Emanuel Peled, School of Chemistry, Tel-Aviv University.

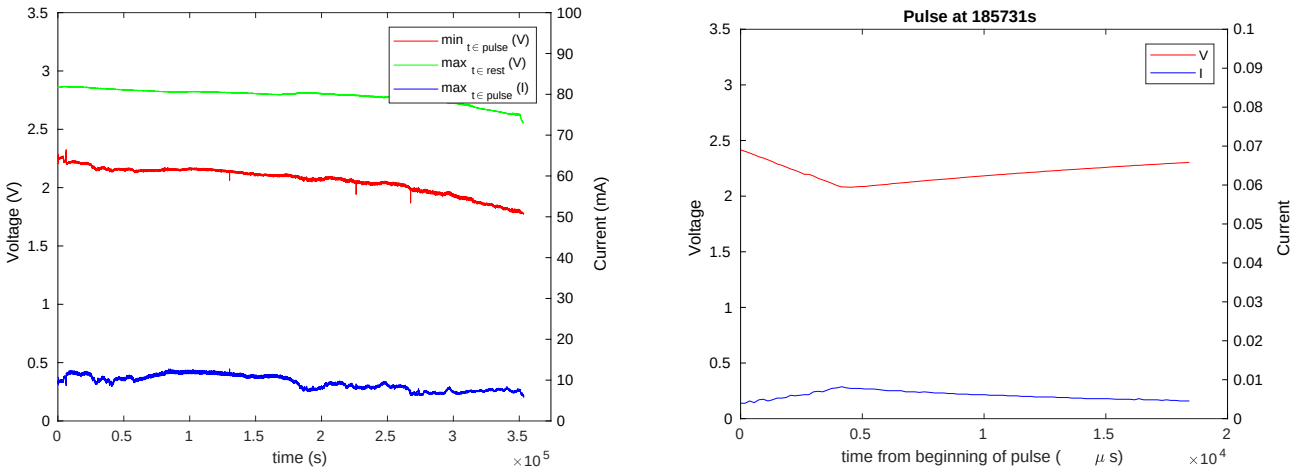

Figure 8: Behavior of a tag powered by a Renata CR1225 battery in parallel with a tantalum capacitor. The graph on the left shows the overall experiment and the graph on the right the behavior during and after one pulse.

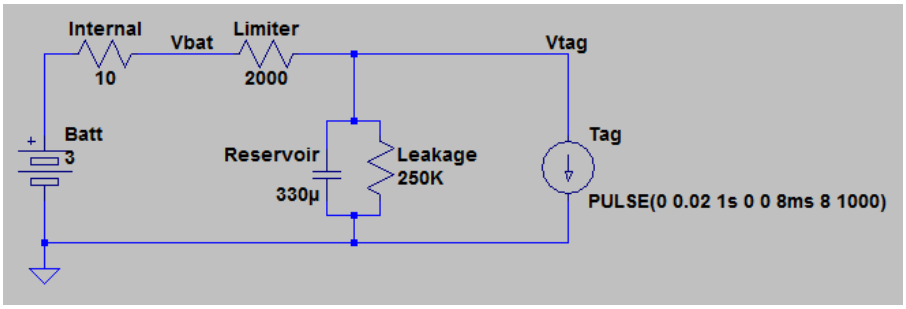

Figure 9: Using a resistor to limit the current sourced from a battery when the tag has a large reservoir capacitor. In this diagram the tag is modeled by a current source, the reservoir capacitor by an ideal capacitor in parallel with a resistor that models leakage, and the battery as an ideal voltage source in series with a resistor that models internal resistance.

5 Limiting Peak Battery Current

To prevent or mitigate concentration polarization, we need to limit from below the impedance that the battery sees, which is equivalent to limiting the current that is sourced from it. This section shows how to do it, evaluates the effectiveness of the solution, and also evaluates the impact of leakage current in the reservoir capacitor. Leakage in large-value capacitors is nontrivial and as we will show, has a significant impact on tags.

5.1 Design Options

There are two main ways to limit the current that is sourced from the battery. One is to connect the battery to the tag and to the reservoir capacitor through a current-limiting resistor, as shown in Figure 9. In this configuration, the tag is powered by the reservoir capacitor; the battery recharges the capacitor after every pulse through the current-limiting resistor. The battery also provides current during a pulse, but it is negligible.

This current limiting configuration raises two concerns. The first is the time it takes to recharge

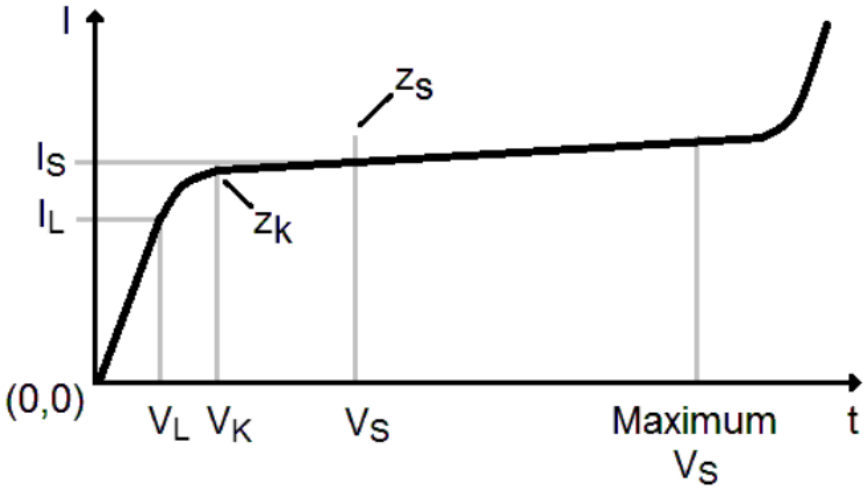

Figure 10: The behavior of typical integrated current regulators from the 1N52XX/1N53XX series. For the 1N5283, for example, $V_L = 1$V,$V_K = 6$V, and the maximum $V_S$is 100V.

the capacitor. During a pulse, the capacitor provides most of the current to the tag, so its voltage drops, because its charge is depleted (the voltage across a capacitor satisfies $Q = CV$ where Q is the charge and C the capacitance). If the next pulse occurs before the capacitor is sufficiently recharged, the voltage at the end of pulses goes lower and lower, possibly causing the tag to shut down or fail. A high-value limiting resistor slows down the recharging, require current-consumption pulses to be less frequent.

The other concern is power wasted in the resistor. We shall see below that the amount of energy wasted on the capacitor is significant but not catastrophic.

The other way to limit current drawn from the battery is with an active current-regulation device. There are integrated current regulators (e.g., 1N5283) or they can be constructed from a transistor (JFET, MOSFET, or bipolar), sometimes with a resistor. An ideal current regulator might have an advantage over a current-limiting resistor because as the capacitor recharges, the impedance of the regulator drops, reducing the amount of energy wasted in it. However, true regulation only starts when the voltage across the regulator is around 1V; below that, the regulator does not conduct or behaves like a resistor. In our case, the regulator rarely sees voltage higher than 1V, so it is not likely to have any advantage. Therefore, we opt for the simpler, physically smaller, and cheaper solution of a current-limiting resistor.

5.2 Simulations

To assess the effectiveness of reservoir capacitors we conducted a series of simulations using LTSpice, a circuit-simulation program. We note that we have also observed the same behaviors on an oscilloscope and using our characterization system. However, extracting quantitative parameters is easier in a simulator. The simulations allow us to correctly size the current-limiting resistor and to estimate the energy wasted on both the current-limiting resistor and on leakage in the capacitor.

The general setup for the simulations is shown in Figure 9. The value of the capacitor is 330μF,

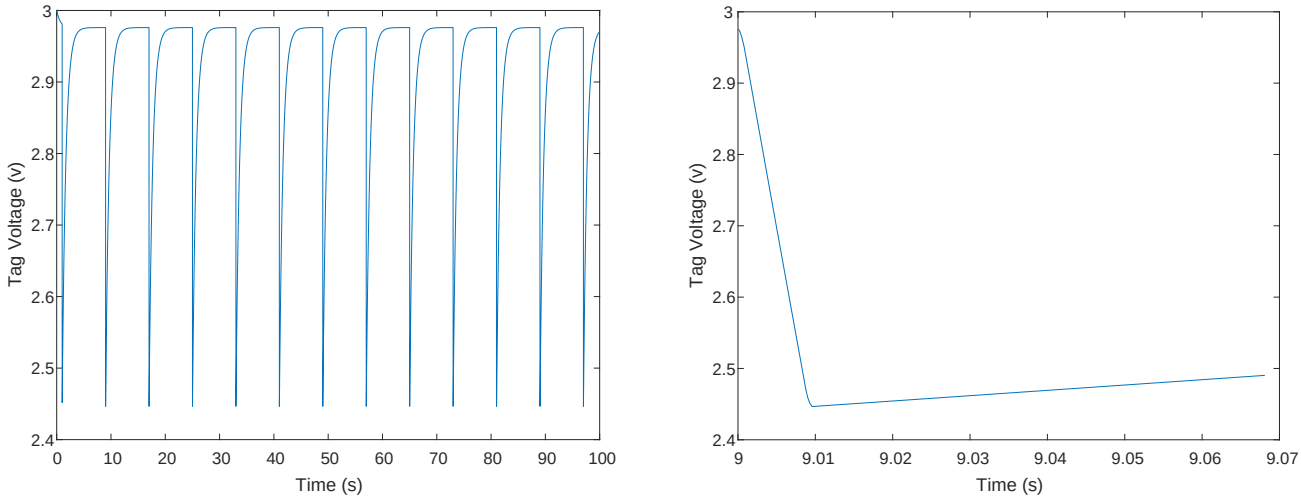

Figure 11: A 100s simulation of the circuit shown in Figure 9. The tag (current source) sank 20mA for 8ms every 8 seconds. On the right we see the entire 100s, showing that between current-sinking pulses, voltage on the capacitor reaches an asymptote close to 3V. On the right we see the voltage during and after one pulse. During the pulse, it drops almost linearly due to the $Q = CV$ behavior of the capacitor and the almost linear decrease in charge Q. After the pulse, voltage starts to rise as the capacitor is discharged through the current-limiting resistor.

the actual value we use. The value was selected to allow 8ms, 30mA pulses starting from 3V and ending at a safe margin away from the 1.8V limit of the RF microcontroller (the margin also takes into account the 20% tolerance of the capacitor). The leakage is modeled by a 250k resistor. The actual leakage is specified as 20.8μF at 6.3V and at 20C, rising by a factor of at most 10 at 85C (leakage rises with temperature).

Figure 11 shows the voltage on the tag when the battery is connected through a 2k resistor. During each 8ms current-consumption pulse the voltage on the capacitor (and on the tag's electronics) drops as the capacitor is discharged. The drop is almost linear because the current provided by the battery during the pulse is insignificant. Between pulses the capacitor is discharged, here all the way to an asymptote at 2.976V. That value is a little lower than 3V because of the voltage divider formed by the three resistors.

Figure 12 shows what fraction of the energy drawn from the battery is spent on the tag and what fractions are wasted on the current-limiting resistor and on leakage, as well as the minimal voltage seen by the tag. The voltage levels are safe down to an inter-pulse interval of 1 or even 0.5s. The amount of energy wasted is minimized at inter-pulse intervals of 1s to 2s, where is it around 20%. At shorter intervals, a significant fraction of the energy is wasted in the current-limiting capacitor. At long intervals, the energy wasted on leakage becomes significant, reaching almost 50% at 16s. The energy spent on the limiter drops a little at long intervals, but not significantly. The non-monotonic shape of the graph of productive energy expenditure suggests that the limiting resistor should be sized according to the inter-pulse interval.

Figure 13 presents a series of simulations designed to help select a current-limiting resistor for a tag that transmits a 8ms 20mA pulse every 2 seconds. The graphs show that the best efficiency, around 80%, is achieved with resistors in the 1k to 2k range. Even a 4k resistor, which protects the battery even better, is plausible; efficiency is 76% and the minimal voltage is 2.3V. At 8k, the

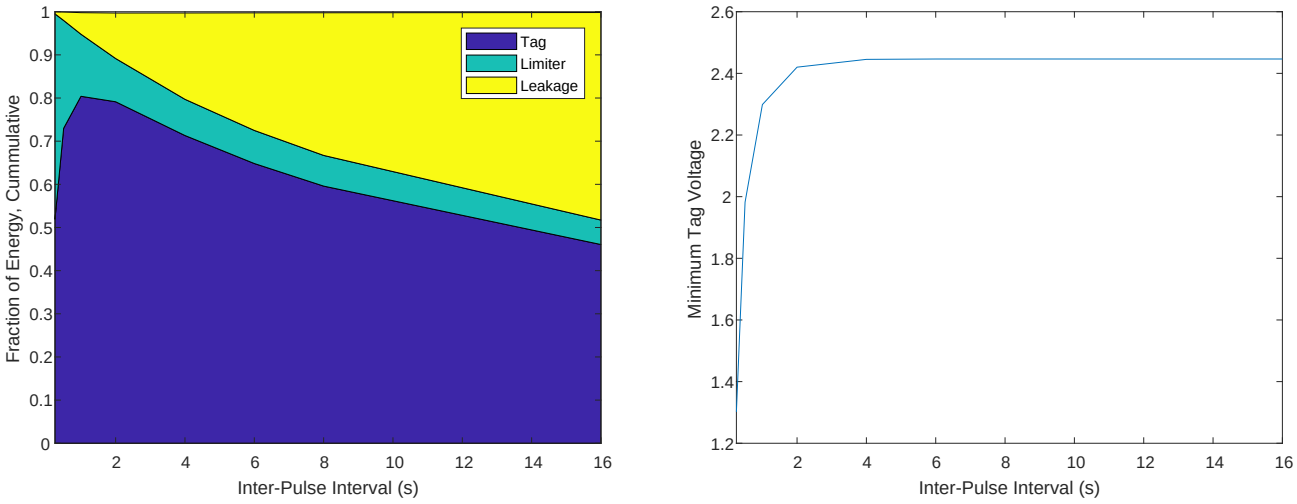

Figure 12: The distribution of battery energy and the minimal voltage seen by the tag in simulations of the system with different inter-pulse intervals. The other parameters are the same as in Figures 11 and 9. The minimal voltages at short inter-pulse intervals are a little difficult to read from they graph; they are 2.3V at intervals of 1s, 2.0V at 0.5s, and 1.3V at 0.25s.

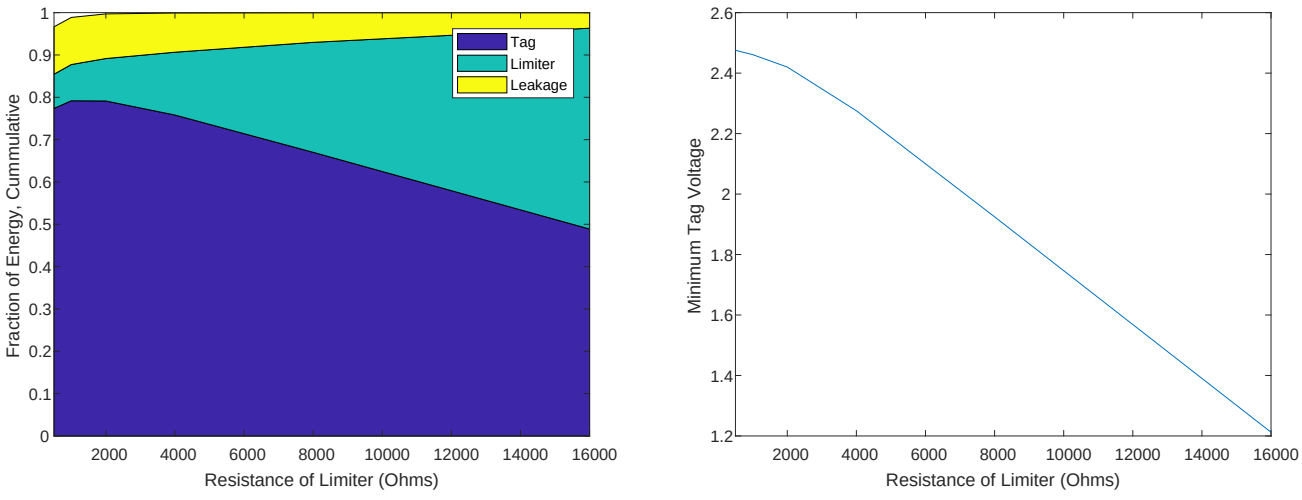

Figure 13: The same quantities plotted in Figure 12, but as a function of the current-limiting resistor. The inter-pulse interval was 2s in all cases. At the low-resistance end, the fractions do not sum to 1, most likely due to numerical errors in the circuit simulator.

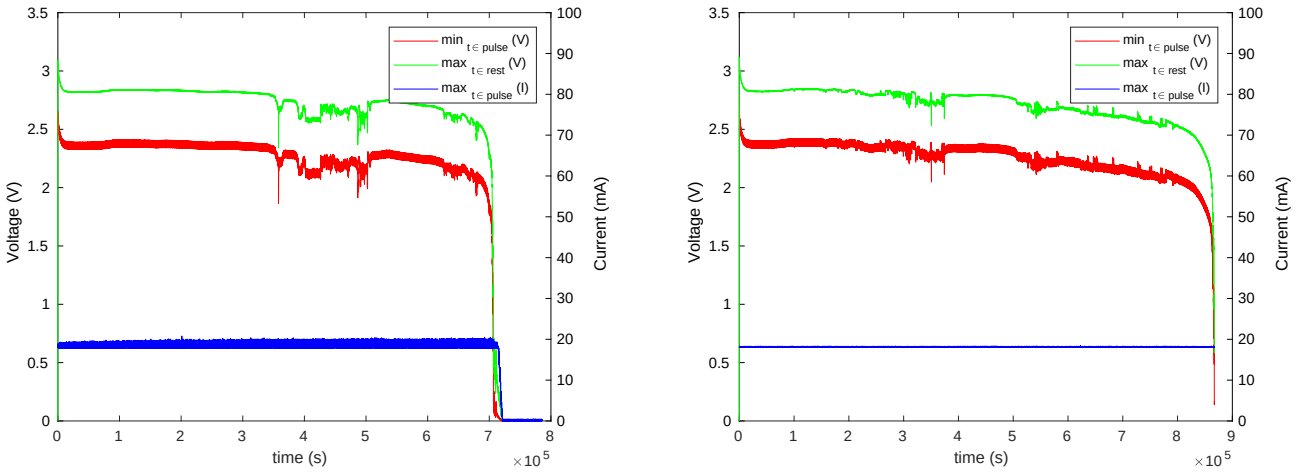

Figure 14: The results of a pulsed current-consumption experiments (20mA for 8ms every 1s) when CR1025 batteries were connected to a 330μF tantalum reservoir capacitor through a 1k resistor.

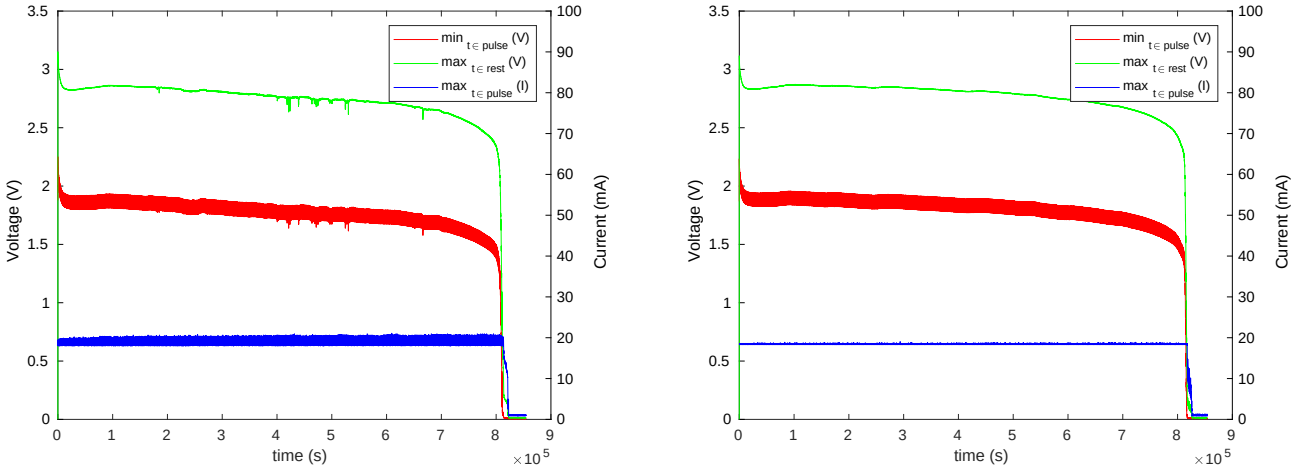

Figure 15: The results of a pulsed current-consumption experiments (20mA for 8ms every 1s) when CR1025 batteries were connected to a 330μF ceramic reservoir capacitor through a 1k resistor.

minimal voltage is 1.9V, too close to the 1.8V threshold and efficiency drops further to 67%.

5.3 Experimental Results

To explore the effectiveness of the current-limiting resistor in mitigating concentration-polarization failure, we ran 4 more experiments with Renata CR1025 batteries from the same batch, all connected to a reservoir capacitor through a 1k resistor. Two were connected to ceramic capacitors (330μF nominal, about 220μF effective) and two to 330μF tantalum capacitors. The results are shown in Figures 14 and 15. The experiments with tantalum capacitors, still showed some transient voltage drops, but much less than the experiment without a resistor (Figure 6). There was also a significant different in the lifespans of the two batteries, perhaps as a result of the these transient failures. The experiments with ceramic capacitors showed no significant voltage drops. The only relevant difference between the two setups is the effective capacitance and we are not sure what caused the difference in behaviors.

To determine whether a larger resistor and larger inter-pulse periods would prevent the transient failures with tantalum capacitors we repeated the experiment but with two 3.3k resistors and with 4s inter-pulse intervals. The results included significant transient voltage drops in some of the experiments, suggesting that the current-limiting resistor, at least at these resistances, reduces concentration polarization but does not eliminate it completely. We address this finding in Section 7 with an additional mitigation mechanism, but before that we show how to size the reservoir capacitor and the current-limiting resistor.

5.4 A Design Procedure

We propose the following procedure to select the reservoir capacitor and the current limiting resistor. The capacitor is typically placed on the tag's printed circuit board (PCB), so it should be selected when the tag is designed. If a larger capacitor is required in some applications (e.g., applications requiring longer pulses), the extra capacitor can be soldered to the one on the board. The resistor can reside on the board (we normally include one in our tags, but its value may not be optimal for all tag configurations), but a small through-hole resistor can also be used in lieu of a wire connecting the battery to the board. Replacing a small resistor on the board is difficult, because of the size (the bulk capacitor much larger).

Sizing the capacitor starts with a conservative estimate of the total charge sank into the tag during a pulse of activity. This can be estimated by measuring the current that a prototype tag (e.g., an evaluation board running the tag firmware) consumes during a pulse, as well as before and after the pulse, if these are significant. The current can be measured using a current-sensing resistor and an oscilloscope, or using the current-sensing circuitry that is built into some evaluation boards of RF microcontrollers . Obviously, the current can also be measured using our characterization system, when used in logging mode.

The charge can also be estimated from data-sheet information, and it is prudent to use that approach even when direct measurements are made, to ensure that the measured data conforms to the data-sheet specification. These calculations are not always trivial, so we demonstrate them using an example. The CC1310 that is used on our tags [12] is specified to consume 13.4mA when transmitting a 10mW radio signal, when the device is powered by a 3.6V source, and when the device uses its DC-DC switching regulator. Because of the switching regulator, the CC1310 consumes roughly constant power during the pulse; the information in the data sheet specifies the power as $13.4 \times 3.6 = 48.24$mW. Therefore, during an 8ms pulse the tag consumes 0.386mJ. The energy in a capacitor is $E = (1/2)CV^2$, so the voltage V_{end} at the end of the pulse satisfies

$$\frac{1}{2}CV_{\text{start}}^2 - 0.368 \times 10^{-3} = \frac{1}{2}CV_{\text{end}}^2 ,$$

where V_{start} is the voltage on the capacitor at the beginning of the pulse (hopefully the voltage of the battery when it is not under load). If we assume that $V_{\text{start}} = 3$ and we constrain $V_{\text{end}} \geq 2.4$,

for example, we obtain

$$\begin{aligned} V_{\text{end}}^2 &= V_{\text{start}}^2 - \frac{2\times 0.368\times 10^{-3}}{C} \\ &= 9 - \frac{2\times 0.368\times 10^{-3}}{C} \\ &\geq 2.4^2 \\ \frac{2\times 0.368\times 10^{-3}}{C} &\leq 3.24 \\ C &\geq \frac{2\times 0.368\times 10^{-3}}{3.24} = 227.16\mu\text{F}\,. \end{aligned}$$

If the same CC1310 chip is configured to use its linear regulator, not the switching regulator, the calculation is carried out a little differently. Both regulators output about 1.7V, so when producing a 10mW RF output, the device consumes about 48.24mW/1.7V = 28.38mA. When a linear regulator is used, the device consumes this much current at all voltages (the device behaves like a constant-current sink). Therefore, during an 8ms transmission the amount of charge consumed from the reservoir capacitor is 28.38mA × 8ms = 0.227mC. Using the $Q = CV$ capacitor equation we find that

$$\begin{aligned} Q_{\text{end}} &= Q_{\text{start}} - 0.227\text{mC} \\ CV_{\text{end}} &= CV_{\text{start}} - 0.227\text{mC} \\ &= C\times 3 - 0.227\text{mC}\,. \end{aligned}$$

We can again solve for the limit on C,

$$\begin{aligned} V_{\text{end}} &= 3 - \frac{0.227\text{mC}}{C} \\ &\geq 2.4 \end{aligned}$$

or

$$C \geq \frac{0.227}{3-2.4} = 378\mu\text{F}\,.$$

Next, the value of the resistor should be selected using the simulation shown in Figure 9. The appendix shows the Spice directives that extract the relevant parameters from the simulation.

6 Preventing Reservoir-Capacitor Leakage

Unless the tag transmits or performs other high-power activity often, much of the battery energy is wasted due to leakage in the reservoir capacitor, as shown in Figure 12. We have not found low-leakage alternatives. Therefore, in tags that transmit infrequently (less than about every 8s) and in tags that are in storage (inactive), it is better to disconnect the reservoir capacitor during times of low current consumption, to prevent leakage.

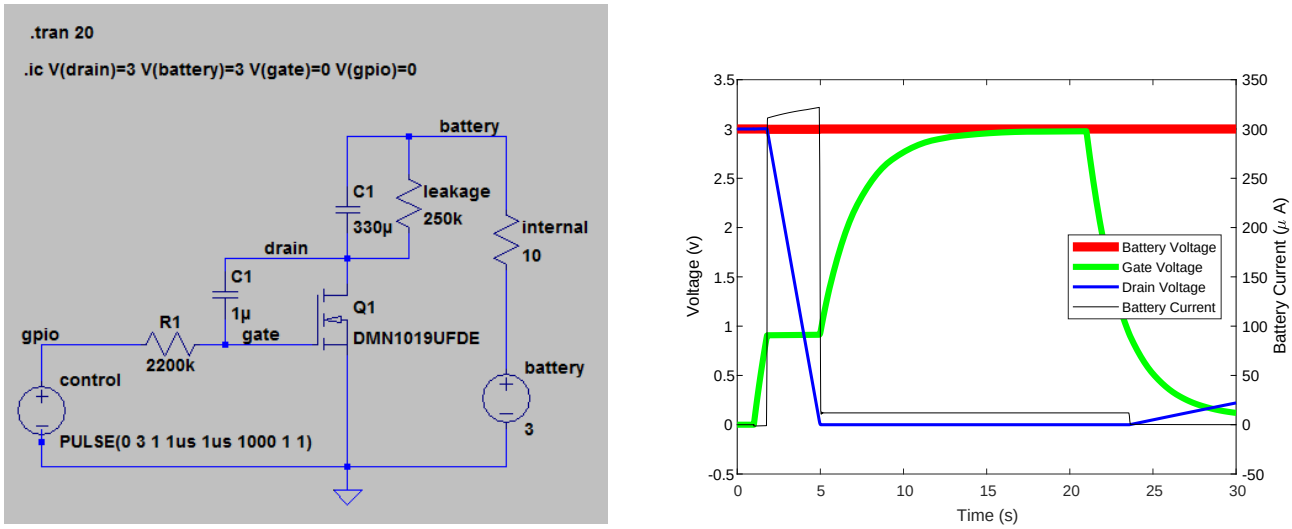

Figure 16: Using an artificial Miller effect to slowly charge the reservoir capacitor. Left: the slow-start circuit, here part of an LTSpice simulation. Right: the results of the simulation. Control voltage starts at 0, transitions to 3V at 1s, then back to 0 at 21s. Oscilloscope traces show the same behavior.

Disconnecting the capacitor is fairly easy, using a power MOSFET. This increases the size of the tag due to the additional component, but not by much. However, reconnecting the capacitor requires a careful design. If we reconnect the capacitor with a digital signal that turns the MOSFET on, the charging current of the capacitor will crash the voltage that the tag sees and will cause the tag to reset. This will happen whether a current-limiting resistor is used or not.

6.1 A Slow-Reconnect Mechanism

To avoid this, we designed a simple analog circuit that charges the capacitor slowly, so as not to crash the battery's voltage. The circuit is shown in Figure 16. When the tag is in sleep mode, the control voltage is 0, transistor Q1 is turned off, and the reservoir capacitor C1 is discharged, so the drain voltage is identical to the battery's voltage, 3V. When the microcontroller decides to enable the reservoir capacitor, it turns the control voltage on (to 3V) and waits 5 seconds. To disable the reservoir capacitor and the leakage that it causes, the microcontroller turns the control voltage off.

The results of a simulation of a turn-on and a turn-off events is shown in Figure 16 (right). The simulation starts with the capacitor disconnected. The control voltage and the gate voltage are 0 and the voltage at the drain is 3V, the same as the battery voltage. This simulates the state of the circuit after all the charge in C1 has leaked. At this state, C2 is charged, and there is no current flow in the circuit. When the control voltage rises to 3V one second after the simulation starts, the voltage at the gate gradually rises to about 0.9V, then plateaus, then rises to 3V. During the plateau period, voltage at the drain drops close to linearly as the reservoir capacitor is charged with close-to-constant current. While the transistor is on, about 12μA leaks through the capacitor. When the control voltage is turned off, C2 is charged through R1, which causes the gate voltage to drop until the transistor stops conducting. At that point, drain current starts rising due to leakage

in C1, but there is again no current flowing out of the battery.

The behavior of the gate voltage at turn-on is a slowed-down version of the normal behavior of a MOSFET that is turned on by a fast rising edge at the gate (see, e.g., [13]. The normal (and much faster behavior) is caused by the gate resistance R_g and the gate-drain capacitance C_{gd} that are parasitic elements in any MOSFET. In our circuit these parasitic resistance and capacitance are augmented by the large R1 and C2, slowing down the transition.

The utility of this circuit (and in particular, of the large R1 and c2) is that it charges the reservoir capacitor at an almost constant current whose magnitude depends on the length of the plateau (called the Miller plateau in discussions of MOSFET behavior), which in turn is controlled by the *RC* product of R1 and C2. That is, we can keep this voltage low, so as not to drop the battery voltage below 1.8V, by selecting large R1 and C2.

6.2 Software Control of the Mechanism

In our tags, we use an ultra-low-power core to control this mechanism. The tags use a CC1310 RF microcontroller, which has three processing cores: a general purpose ARM Cortex-M3 CPU, an ARM Cortex-M0 CPU dedicated to operating the radio, and an ultra-low power core called a *sensor controller*. In our firmware, the sensor-controller implements a state machine with the following states.

- The initial state, state 5, in which the reservoir capacitor is charging and the control voltage is on. When entering this state, the code sets up a timer event in When the timer expires, the state machine sets up an interrupt on a pin connected to a Hall sensor. When the interrupt arrives and transitions to state 1.

- A transition to state 1 signifies that an external event signals that the user wants to put the entire system to sleep. This is achieved by placing a magnet near the tag, which activates a low-power Hall sensor. The state machine sends an interrupt notification to the Cortex-M3 core, indicating that it should stop all activity. The state machine waits for an interrupt from the Cortex-M3; when it arrives, it transitions to state 2.

- The interrupt that caused the transition to state 2 signals that the Cortex-M3 has stopped its activities and is in sleep mode, so the reservoir capacitor can be disconnected. The control voltage is set low, to disconnect the MOSFET. The state machine waits for an interrupt indicating that the magnet has been removed, which signifies that the user wants the system back on.

- The interrupt causes a transition to state 3, in which the control voltage is set back high. The state machine waits 10s for the capacitor to charge, then transitions to state 4.

- In state 4 the state machine sends an interrupt to the Cortex-M3, indicating that the capacitor is connected and charged, so the Cortex-M3 can resume normal tag operations. An interrupt sent back will transition the state machine to state 5.

- When the Cortex-M3 starts, it sends an interrupt back to the sensor controller, which transitions to state 5. It configures an interrupt on the output of the sensor Hall, to wait for the next indication from the user that operations should be halted. When the interrupt occurs, the state machine goes back to state 1.

When the sensor controller starts, it sets the control voltage high to connect the MOSFET, waits 10s, and then starts the state machine at state 5.

7 Firmware-Based Prevention of Concentration Polarization

Given our findings that current limiting does not completely eliminates voltage drops due to concentration polarization, we developed another mechanism to prevent tags from resetting or failing when that this happens. This mechanism has two parts, an offline analysis part and an active firmware control part. The offline task is to estimate the maximum voltage drop during an activity period. This estimate can be derived from the equations shown in Section 5.4, allowing for variations in current consumption and in the capacitance of the reservoir capacitor.

The online mechanism that the firmware implements monitors the voltage at the beginning of an activity period. If it sufficiently high to ensure that the voltage at the end of the activity period will remain safely above the reset threshold (1.8V), processing continues normally. If it is not, processing is halted and the system is returned to deep sleep mode. The next wakeup can be scheduled for the next activity slot, but it can also be deferred further, say using exponential backoff, to prevent tag failure due to repeated wakeups that only monitor the voltage and return to sleep. As an example, if we estimate the maximum voltage drop during an activity period to be 0.4V and the reset threshold is 1.8V, we might set the inactivity threshold at 2.3V, giving a 0.1V margin. Monitoring the battery voltage at the beginning of an activity period can be done using an ADC or using a comparator.

To assess the effectiveness of this mechanism, we ran 8 additional experiments that tested this mechanism using an enhanced version of the load-simulation system, in which the firmware implemented this mechanism and was able to report when it caused activity periods to be skipped. All the experiments used CR1025 batteries and 330μF tantalum capacitors. Two experiments used 3.3k current-limiting resistors and inter-activity intervals of 4s; four experiments used 1k resistors and 1s intervals; two used no resistor and 1s intervals.

Six of the experiments showed no transient voltage drops below 2.3V at the beginning of an activity period. Two showed such voltage drops, multiple ones in both experiments. One of these used a 1k resistor and the other no resistor. The results are shown in Figures 17 and 18. The results indicate that the mechanism is effective; supply voltage did not drop below 1.8V even though the batteries did experience voltage drops. The activity periods were not, of course, completely periodic; some were skipped to avoid voltages below 1.8V.

Figure 19 shows the length of these inactivity periods that the firmware imposes to let the battery recover. Towards the end of the life of the battery these periods become more frequeny and longer; an actual tag would be observed to “stutter” during this period. In one experiment

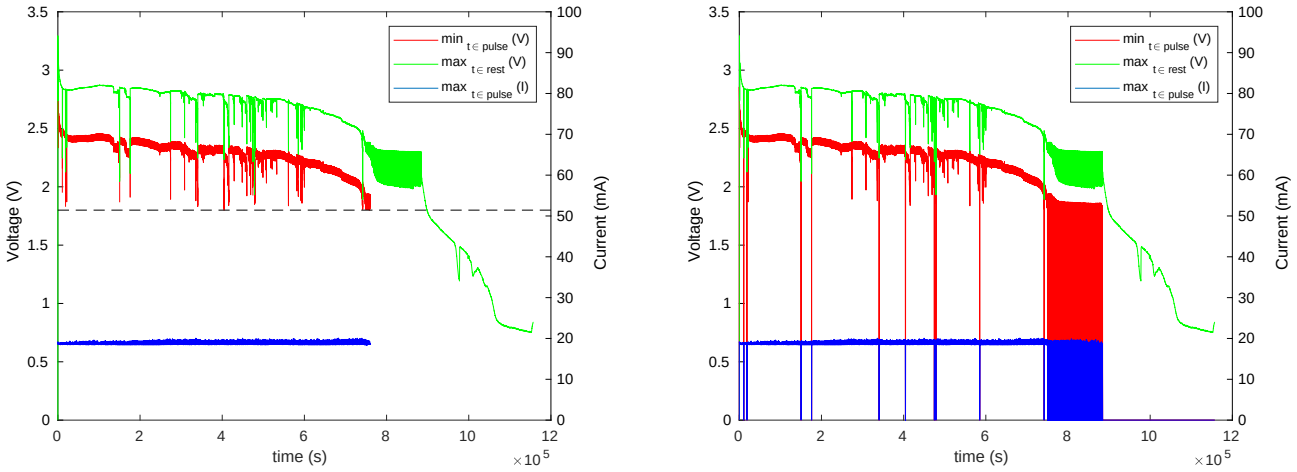

Figure 17: The results of an experiment with a CR1025 battery, tantalum reservoir capacitor, no current-limiting resistor, and with activity-period skipping when the voltage at the beginning of a period is less than 2.3V. The graph on the left shows measured voltages and currents. The graph on the right shows the same data, but with skipped periods represented by 0V and 0A, to show when activity periods were skipped..

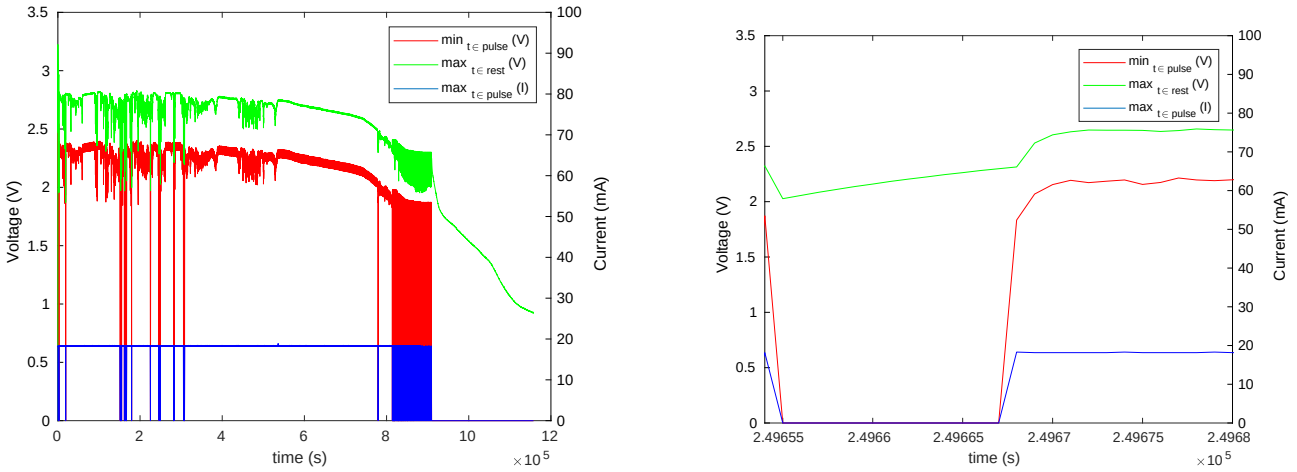

Figure 18: The results of an experiment similar to that shown in Figure 17, but with a 1k current-limiting resistor. The graph on the right zooms in on one contiguous set of skipped activity periods..

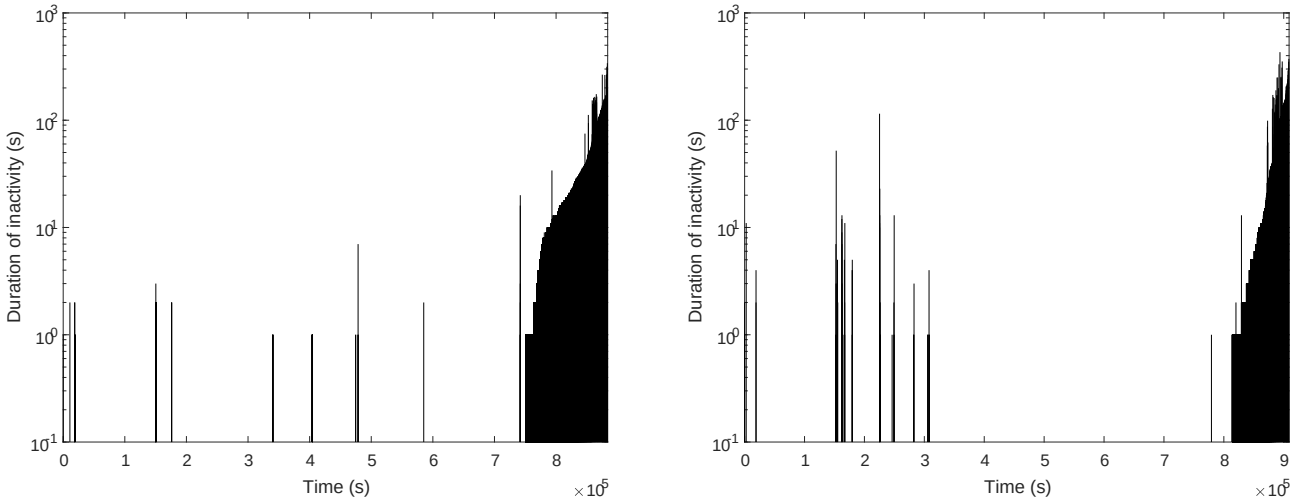

Figure 19: Times at which the load simulator skipped pulses and the duration of the inactivity periods that were required for the battery voltage to rise back above the threshold. The graph on the left shows the result of an experiment with no current-limiting resistor and the graph on the right the results with a 1k resistor.

the periods of inactivity were short as long as the battery was relatively full, up to about 10s, with most periods being shorter. In the other experiment, there were more inactivity periods that lasted 10s or more, and one lasted around 100s.

8 Conclusions

We have demonstrated that small lithium coin cells that are exposed to periodic low- and medium-impedance loads suffer from transients of high internal resistance. This appears to be caused by concentration polarization, an phenomenon of unevenness in the distribution of reactants near the battery's electrode. This happens when the battery powers the electronics directly (a load of about 150Ω for 8ms ever second in our experiments) and when the battery's role is to recharge a reservoir capacitor, both when the battery is connected in parallel with the capacitor and when it is connected to it through a 1kΩ or 3.3kΩ resistor. The inclusion of a current-limiting resistor appears to mitigate the effect but not to eliminate it completely.

This effect can easily cause the microcontroller to reset, or, depending on how quickly the voltage recover, get stuck in an inconsistent state that drains the battery without delivering the required function. The only reliable way that we found to eliminate this risk is to include a reservoir capacitor that stores enough energy to power the circuit during a burst of activity, and to skips such bursts if the starting voltage is low enough to risk a reset.

We have also found that this effect is not particularly rare, but does not happen with every single battery. Batteries, even from the same batch, vary with respect to this effect. This underlies the need to perform rigorous testing on systems powered by such batteries.

Our findings have been made possible by a low-cost, easy-to-use, and easy-to-replicate load simulator and monitor. This load simulator allowed us to perform up to 8 experiments concurrently, all using a single computer and at a moderate cost. Our design is freely available and

should enable others to perform similar detailed analyses of electronic systems powered by miniature batteries and/or by energy harvesting devices.

References

[1] AVX. *F95 Series: Standard Conformal Coated Chip (Tantalum)*, 2018. Data sheet, available online at `http://datasheets.avx.com/F95.pdf`.

[2] Honghao Chen, Samuel Cartmell, Qiang Wang, Terence Lozano, Z. Daniel Deng, Huidong Li, Xilin Chen, Yong Yuan, Mark E. Gross, Thomas J. Carlson, and Jie Xiao. Micro-battery development for juvenile salmon acoustic telemetry system applications. *Scientific Reports*, 4(3790):1–5, 2014.

[3] W. W. Cochran and Rexford T. Lord. A radio-tracking system for wild animals. *The Journal of Wildlife Management*, 27:9–24, 1963.

[4] Z. D. Deng, T. J. Carlson, H. Li, J. Xiao, M. J. Myjak, J. Lu, J. J. Martinez, C. M. Woodley, M. A. Weiland, and M. B. Eppard. An injectable acoustic transmitter for juvenile salmon. *Scientific Reports*, 5(8111):1–6.

[5] Falko Dressler, Simon Ripperger, Martin Hierold, Thorsten Nowak, Christopher Eibel, Björn Cassens, Frieder Mayer, Klaus Meyer-Wegener, and Alexander Kölpin. From radio telemetry to ultra-low-power sensor networks: tracking bats in the wild. *IEEE Communications Magazine*, 54(1):129–135, January 2016.

[6] Mark W. Lund. Battery impedance and resistance, 2000. `https://www.powerstream.com/internal-resistance.htm`, retrieved November 2018.

[7] Thomas L. Martin. *Balancing Batteries, Power, and Performance: System Issues in CPU Speed-Setting for Mobile Computing*. PhD thesis, Carnegie Mellon University, 1999.

[8] B. Naef-Daenzer, D. Früh, M. Stalder, P. Wetli, and E. Weise. Miniaturization (0.2g) and evaluation of attachment techniques of telemetry transmitters. *The Journal of Experimental Biology*, 208:4063–4068, 2005.

[9] Taiyo Yuden. *JMK325ABJ337MM-P: Multilayer Ceramic Capacitors (High dielectric type)*, 2018. Data sheet.

[10] Sivan Toledo. Evaluating batteries for advanced wildlife telemetry tags. *IET Transactions on Wireless Sensor Systems*, 5:235–242, 2015. Appread online; assignment to an issue is pending.

[11] Sivan Toledo, Oren Kishon, Yotam Orchan, Yoav Bartan, Nir Sapir, Yoni Vortman, and Ran Nathan. Lightweight low-cost wildlife tracking tags using integrated tranceive rs. In *Proceeings of the 6th Annual European Embedded Design in Education and Research Conference (EDERC)*, pages 287–291, Milano, Italy, September 2014.

[12] Sivan Toledo, Yotam Orchan, David Shohami, and Motti Charter and Ran Nathan. Physical-layer protocols for lightweight wildlife tags with Internet -of-things transceivers. In *Proceedings of the 19th IEEE International Symposium on a Wolrd of Wireless, Mobile, and Multimedia Networks (WOWMOM)*, pages 1–4, June 2018. work-in-progress paper, to appear.

[13] Vishay. Power MOSFET basics: Understanding gate charge and using it to assess switching performance. Application Note AN608A, Vishay Siliconix, 2016.